

JPMTR 118 | 1903  
 DOI 10.14622/JPMTR-1903  
 UDC 762:777.1|77.02(0.033)

Research paper  
 Received: 2019-02-05  
 Accepted: 2019-03-18

# Assessing and improving edge roughness in pad-printing by using outlines in a one-step exposure process for the printing form

Christina Bodenstein, Hans Martin Sauer, Felipe Fernandes and Edgar Dörsam

Technische Universität Darmstadt,  
 Institute of Printing Science and Technology,  
 Magdalenenstr. 2, 64289 Darmstadt, Germany

bodenstein@idd.tu-darmstadt.de  
 sauer@idd.tu-darmstadt.de  
 doersam@idd.tu-darmstadt.de

## Abstract

We describe the specificities of the pad-printing form production. In printing experiments, we show the influence of different printing forms, in dependence on raster frequency and printing form material, on the printing quality of pad-printed patterns. A typical defect in pad-printing, the ‘stamp effect’, which occurs as a wavy contour, was determined and traced to the printing form production. By incorporating so-called outlines into the printing form, we were able to reproduce patterns with an edge roughness of less than 3  $\mu\text{m}$ . We provide descriptions of the implementation of these outlines. To measure and analyze the edge roughness and edge defects we developed an image-based method to quantitatively assess the quality of edge patterns. With the use of outlines in the printing form, it seems feasible to use pad-printing for source and drain contact manufacturing on printed thin film transistors. Thus, the reproduction of electrically conductive, interdigital patterns for sources and drains having an electrode distance of less than 10  $\mu\text{m}$  appears possible.

**Keywords:** stamp effect, wavy contour, Canny edge algorithm, raster, cliché

## 1. Introduction and background

Pad-printing is often used to print small, high-resolution patterns on curved surfaces. This technology is also known as indirect gravure printing technology since the printing pattern is engraved and the ink in it is picked up by a flexible subcarrier, the pad (Hakimi Tehrani, 2018). The pad is made of elastic, compressible silicone and can thus adapt to curved surfaces. This makes it feasible to print on dye-cast plastic bodies, pre-structured printed circuit boards, 3D-printed rapid prototypes and individually-shaped surfaces (as shown in Figure 1) in a most cost-efficient manner. Moreover, the silicone with low surface free energy permits complete transfer of ink from pad to substrate, leaving a perfectly clean pad for the next transfer sequence. In recent years, new technologies for producing printing forms, such as direct laser engraving, have become available. Alternative gravure patterns beyond the classical gravure cell raster are now possible, tailored to specific applications and printing inks, and these promise substantial progress in printing resolution and quality.

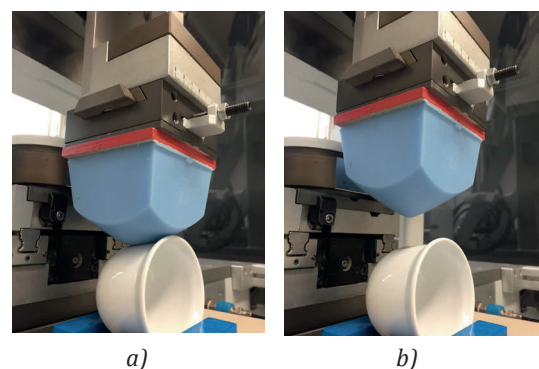


Figure 1: Images of pad-printing on a cup, showing how the flexible pad clings to the shape of the object to transfer the ink (a), and after the transfer moves back upwards and returns to its original form (b)

Particularly for printed electronics, pad-printing is becoming more widely used, with successful applications in solar cells (Hahne, et al., 2001; Krebs, 2009), microwave antennae (Xiong and Qu, 2011), sensor structures (Leppävuori, et al., 1994), UHF RFID (Merilampi,

et al., 2011), electrodes (Mooring, et al., 2005), electroluminescence (Lee, et al., 2010; Bodenstein, et al., 2018a) and source-drain structures (Willfahrt, 2007). Recently works on the pad-printing process itself (Al Aboud, et al., 2018; Hahne, 2001), the pad (Hakimi Tehrani, 2018), and the pad-printed image quality (Hübner and Till, 2007; Bodenstein, 2018; Bodenstein, et al., 2018b) have taken place. Especially in the field of printed electronics it is important to evaluate the printed patterns, since in this area functional materials with electrical properties are used. Instead of pigments or dyes that are responsible for coloring in a common printing ink, particles with electrical properties are used. When printing microstructures the edges play a significant role. Typical defects appearing in pad-printing have to be avoided, such as the ‘stamp effect’ as shown in Figure 2, without changing the electrical properties of the ink to guarantee stable conditions of the printed component.

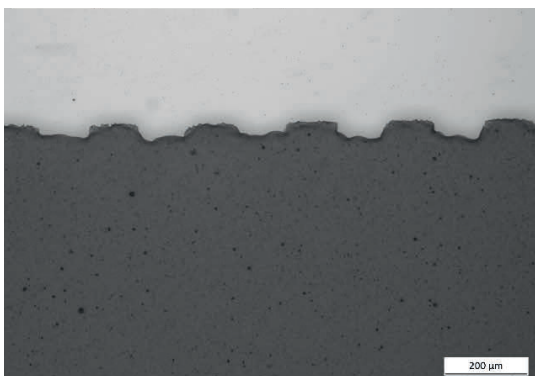


Figure 2: Microscopic image of a typically appearing printing defect in pad-printing – ‘stamp effect’

These defects, which will be discussed in detail later, lead to a dysfunction of the component. Up to now evaluating printed edges was empiric in pad-printing. In this study, we introduce and demonstrate a method that reduces printing defects by evaluating and controlling the edge roughness of pad-printed images.

### 1.1 Pad-printing process

In indirect gravure printing technology, the printing layout is engraved as a raster of microscopic cells on a planar printing form or a cylinder. The size of these cells, usually a few tens of micrometres in width and depth, determines the amount of ink transferred to the surface of the substrate. The pad-printing process is shown in Figure 3. After the engraved cells are filled with ink and excess material is removed by blading, which is done by moving the printing form carrier (a), a soft silicone pad is pressed against the printing form (b). When the pad is lifted from the printing form, it takes the ink out of the cells (c), and after moving the printing form carrier back (d) deposits it on the surface of the substrate (e, f).

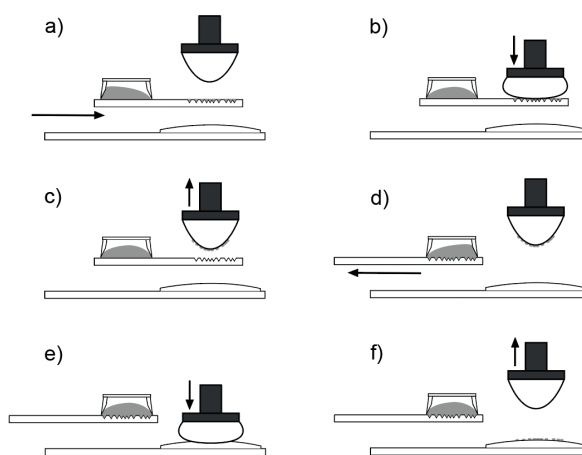


Figure 3: Schematic of the pad-printing process

### 1.2 Pad-printing form ( cliché )

In literature pad-printing technology is rarely described as well as the production of the printing form, which is also called cliché. Pad-printing technology is still a niche technology which is often located in screen-printing companies due to its similar products. The materials that are mostly used for clichés are polymer and steel. The choice of the material depends on different requirements, such as the amount of print runs of each print job, the printing quality, chemical resistance and costs. Each material requires different image processing technologies, such as an UV exposure with an image film for polymer clichés (Section 1.4) or an etching process for steel material (Section 1.5).

Although pad-printing is an indirect gravure printing due to its principle that the ink is transferred from engraved cells, the mainly used printing form production process of polymer cliché itself is based on the same principle as it is in flexographic printing form production.

Even nowadays in 2018, in a digitalized world, printing form production using a film is still the most widely used process in pad-printing industry, as due to its simple and cost-effective process printing companies are fast in operating and self-sufficient from printing form producing companies.

### 1.3 Raster in pad-printing clichés

In printing technology colors are reproduced by printing several single dots (raster dots) with a specific distance with primary colors (CMYK) as described, e.g., in Nisato, Lupo and Ganz (2016). In pad-printing technology the raster has more widely spaced and variable raster components for various reasons. Especially when printing large scale areas, the remaining walls

in between the raster cells have a special importance, similar as in gravure printing technology:

1. In large scale areas the raster functions as a supporting structure. The walls that remain in between the raster cells prevent the blade from tilting into the indentations when blading the excess printing ink material (Figure 3a).
2. The ink would remain unsteady, changing thickness in the indentations. The walls hold back the printing ink homogeneously (Figure 4).
3. When the pad is moving downwards to take the ink out of the indentations, the pad is displacing the ink by its pressing force and rolling motion. The walls are bracing the pad so the pad cannot displace the ink and a homogeneous film can be realized (Figure 5).



Figure 4: After the blading process the ink remains unsteady in the indentations without raster (a), with a raster the walls hold back the ink homogeneously (b)

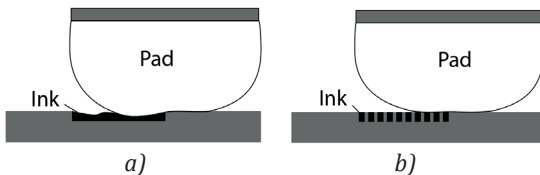


Figure 5: Pad pressing on printing form without raster displaces the ink (a), whereas the walls of the raster brace the pad and the ink is not displaced (b)

### 1.4 Production of photopolymer cliché

Hereafter, the ‘engraving’ process of a polymer cliché with a two-step exposure will be described first, as it is the most widely used material and process for pad-printing forms.

Figure 6 shows the structure of a photopolymer printing plate. A steel base plate (thickness of approx. 300 µm) acts as a stabilizer and carrier, which can be later fixed in the pad-printing machine by magnets. The base plate is connected to the polymer material (thickness of approx. 200 µm) by a bonding layer. A protective layer (thickness of approx. 50–100 µm) prevents mechanical damage and protects the polymer from dust and trapped air (Hahne, 2001).



Figure 6: Photopolymer printing plate structure

Figure 7 shows step by step the process of imaging of polymer pad-printing forms in a so-called ‘two-step exposure’. With the help of an iron-doped metal halide lamps (burner) it is possible to render the photopolymer layer by a complete UV light pre-exposure in a first step (1). The photopolymer material cures from bottom to top and the cured layer thickness gains with longer exposure duration, which controls the depth of the (later developed) cells (Hahne, 2001). A shorter exposure leads to deeper raster cells.

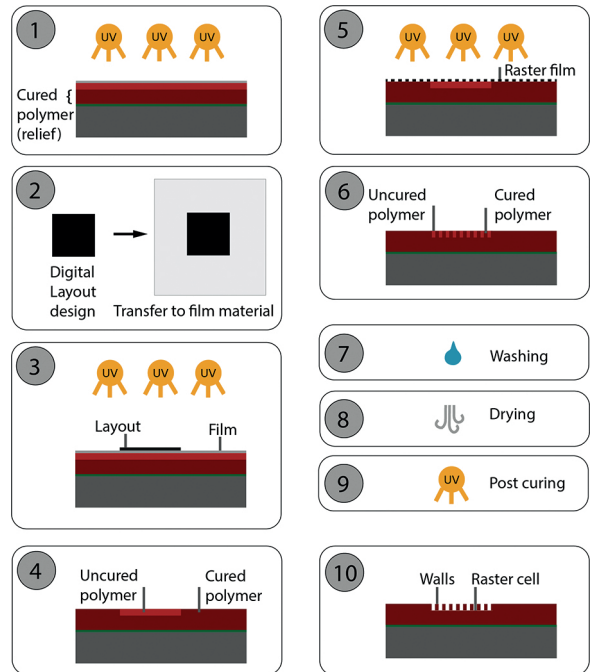


Figure 7: Schematic of polymer pad-printing form production process for a two-step exposure

The printing layout in general is designed with a software, for example Adobe Illustrator. As shown in Figure 7, the digital layout is then transferred to a film material (2). An inverted matted film positive is required with an optical density  $D$  of the black parts of at least  $D = 3.5$  and less than  $D = 0.05$  for the transparent areas (Hahne, 2001). With a too low-density of the black parts UV light can pass through and leads to undesired polymerization. After the protective layer is removed from the photopolymer material, the imaged positive film is then placed on top of the light sensitive polymer material and the 1<sup>st</sup> exposure follows (3). After the exposure the uncovered areas are cured and the areas covered with the black parts of film are still light sensitive (4).

In the next step illustrated in Figure 7, a film that is fully covered with the desired raster dots at specified frequency and area coverage is applied to render the raster cells and the 2<sup>nd</sup> exposure step follows (5), where the UV light passes through the uncovered areas

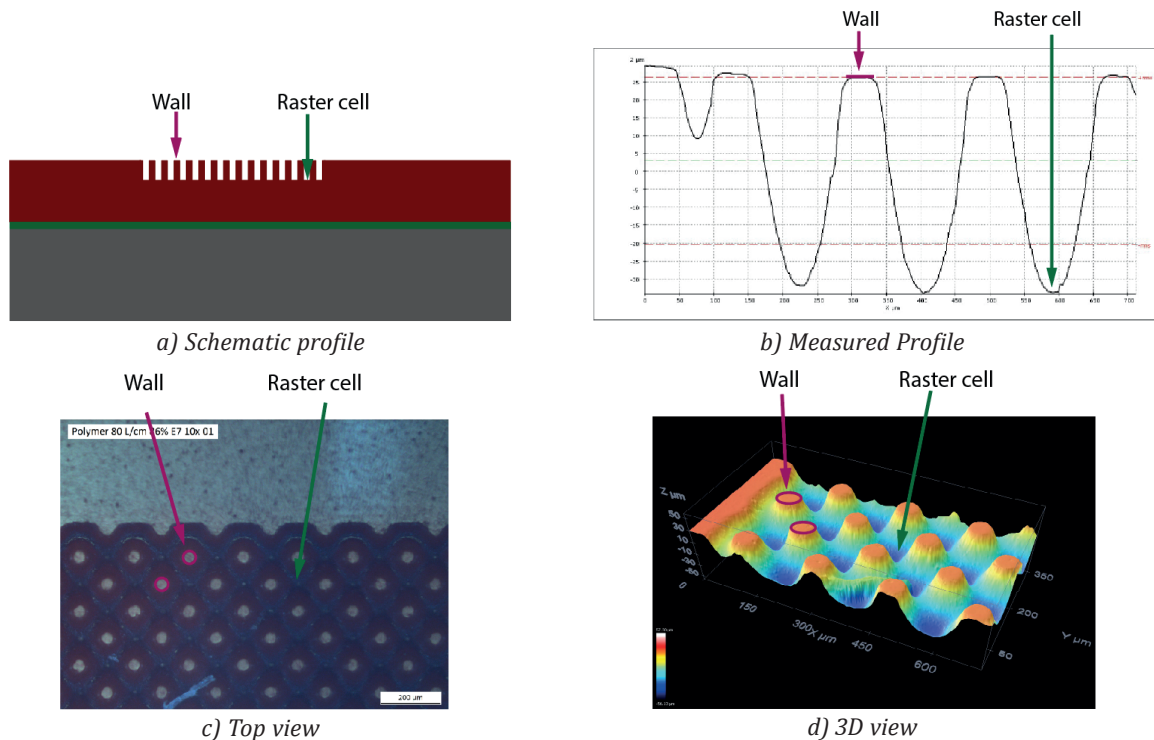


Figure 8: Schematic profile of a pad-printing form (a); the measured profile measured with Sensofar PLu neox (b); the top view taken with Leica DM4000M microscope (c); and the 3D view taken with a Sensofar PLu neox (d) of a pad-printing form with a raster frequency of 80 L/cm and an area coverage of 86 %

and cures the walls (6). After that, the uncured areas need to be washed out with a plush brush by hand or a machine (7). In a drying process (8) the drying agent is evaporated and thus the final hardness of the plate is achieved. To stabilize the walls a post curing is needed (9). Afterwards the cliché is ready to print (10).

Figure 8 shows images of the cells of one finished polymer printing form with a raster frequency of 80 lines per centimeter (L/cm) and an area coverage of 86 %. In all four images the walls and the raster cells are marked. In the printing process the ink remains in the raster cells after the blading process (see Figure 3a), and the walls act as a support structure for the blade (see Section 1.3).

### 1.5 Production of steel strip cliché

Another commonly used material for pad-printing forms is strip of thin steel. The thickness of the flat steel material is 1 mm. This material can achieve longer service life (around 500 000 print runs) than photopolymer (around 20 000) due to higher abrasion resistance. The production compared to photopolymer cliché is more complex and requires special equipment as well as the corresponding disposal system for the produced waste (Lake, 2017). A thin photopolymer layer is coated onto the steel material. This layer is exposed with a film that carries the image information. The areas, that

are not cured are washed out. In the following etching process step the remaining areas, that carry the image information, are then etched into the material with iron(III)-chlorid. Afterwards the etching liquid need to be removed and the material cleaned (Hahne, 2001).

## 2. Materials and methods

### 2.1 Experiments

The pad-printing machine used in the experiments is based on the machine described by Hakimi Tehrani, Dörsam and Neumann (2016) and Hakimi Tehrani (2018). We modified it, by replacing the pneumatic drives of the gravure plate and pad holder by linear stepper drives. These drives were controlled via a National Instruments LabVIEW program. This allows for independent control of each motion of the printing process in distance and velocity, thus making this machine a unique research platform for process evaluation. To increase the versatility of our setup, we also installed force sensors. This enables independent control of each motion by setting forces instead of positions.

We used a chessboard printing pattern with 64 squares, each with an area of 4 mm × 4 mm (Figure 9). Each square is assigned a column (A–H) and row (1–8) iden-



tifier. In the printing process the position of the top of the pad to take out the ink is in the centre of the layout (in-between D4, E4, D5 and E5). In this study we only evaluate the printing tests of the upper edge of square C2, which is a square that is not in the inner parts (close to the pad centre) and not at the outer parts of the layout, as shown in Figure 9.

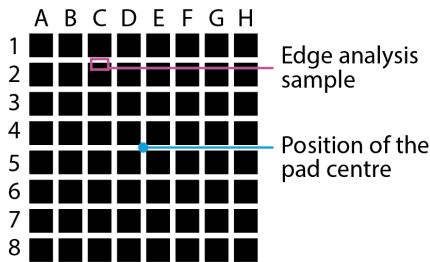


Figure 9: Printing layout and field C2 as edge analysis sample with pad centre position

We used printing forms made of polymer and steel with raster frequencies of 80, 100, and 120 L/cm and area coverage of 86 %. The printing plates are from ITW Morlock GmbH. We chose solvent-based printing ink from Marabu GmbH & Co. KG, type TPL 489 (black) due to its universal applicability on a big variety of materials. The ink is blended with a suggested amount of volume fraction of 20 % of solvent (TPV) to adjust the viscosity. The antistatic pad (TP082, blue, 12 Shore A with the dimensions of 67 mm height, 84 mm × 74 mm ground plate) is from Tampoprint AG and is shown in Figure 10; the substrate is a 125 µm PET Hostaphan GN 4600 foil from Pütz GmbH + Co. Folien KG. The velocities of all moving parts in printing machine, such as movement of the cliché table, as well as of the pad (see Figure 3), were set to 200 mm/s.



Figure 10: Printing pad TP082 used in this study

## 2.2 Edge recognition

To use an automatic edge-recognition software algorithm on printed patterns, one must precisely map a three-dimensional feature onto a continuous line, as shown in Figure 11. This results in a printed three-di-

mensional layer, with edges on top or in direct contact with the substrate. The critical edge which is used for edge evaluation in this work is specified in Figure 11.

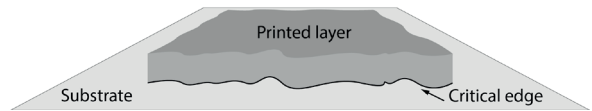


Figure 11: Schematic of the three dimensions of a printed layer; the edge to be investigated is the contact line between the printed layer and the substrate (critical edge)

After the printing process, it is likely that the edges are not perfectly even (Figure 11). On top of that printing defects are occurring. The most critical of these defects are those found at the edges: thin ink bridges that extend beyond the desired border. Without controlling these defects on conductive patterns, they lead to a short circuit between adjacent electrodes. Thus, in printed electronics, it is especially important to precisely evaluate the resolution of printed microstructures. To evaluate this critical edge, we take microscope images from the top view of the printed samples to map the three-dimensions onto a plane to detect the edge. To characterize height profiles, we adapted the roughness measures used in surface technology, as illustrated in Figure 12. Here,  $y_i$  is the center line and  $d_i$  is the distance from a peak to the center line. We applied this procedure to the top view of the border lines of the printed samples, which were measured by optical microscopy. By applying digital contrast amplification, thin ink bridges and residuals can be observed, regardless of the printed layer's local thickness.

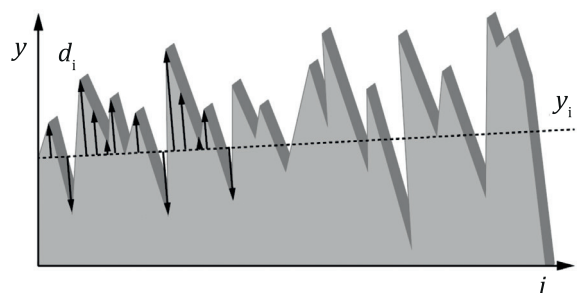


Figure 12: Schematic of roughness measure for height profiles

In this work, the edge roughness is defined as  $R_m$ , the average absolute distance between the desired border line and the actual border line. This is calculated via equation [1] and is used as an edge roughness and blurring measure.

$$R_m = \frac{1}{n-1} \sum_{i=1}^n |d_i - y(i)| \quad [1]$$

With  $n$  we denote the number of measuring points from  $y_i$  to each  $d_i$ . A perfect edge sharpness is  $R_m = 0 \mu\text{m}$ . For  $R_m > 0 \mu\text{m}$  we talk about edge roughness. For the digitalized measurement analysis, we implemented an algorithm using Matlab software. The initial aim of the algorithm is to detect the straight center line  $y_i$ , i.e. the regression line, and the actual printed critical edge, for purposes of calculating  $R_m$  as described in Equation [1]. Printed patterns were determined using a digital Leica microscope DM4000M camera image with a tenfold magnification objective lens. The pictures have the dimensions of  $2592 \times 1944$  pixels ( $219.5 \text{ mm} \times 164.6 \text{ mm}$ ).

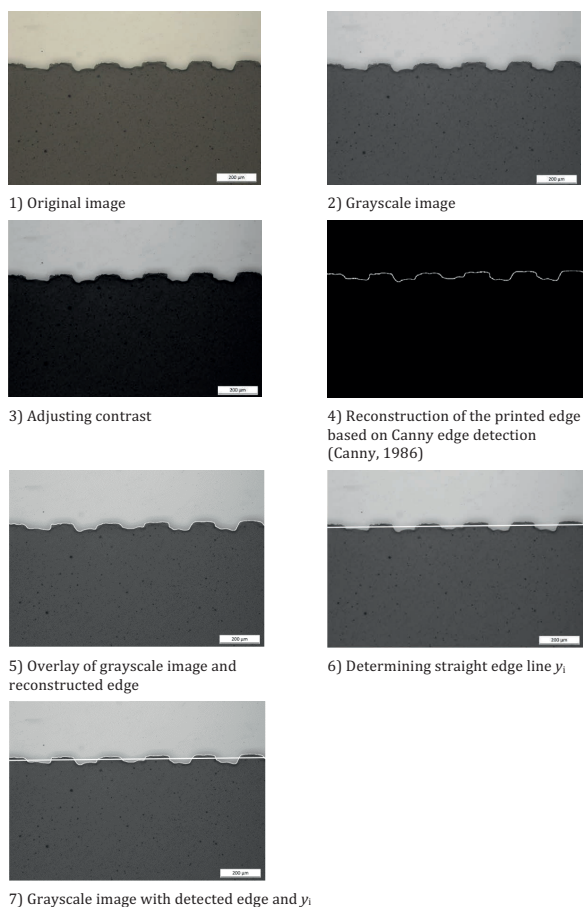


Figure 13: Steps of image processing for determining straight edge line  $y_i$  and average roughness  $R_m$  at field C2 (see Figure 9)

The algorithm we developed to analyze printed edges works as follows. As shown in Figure 13, the acquired RGB image (1) is converted to an 8 bit grayscale image (2), with gray levels between 0 (black) and 255 (white). The image contrast is adjusted such that 1 % of the data has a gray value of 0, whereas the top 1 % of the data has a gray value of 255. This yields a more robust edge distinction (3). The edge of the printed image is detected using a Canny edge algorithm

(Canny, 1986). Compared to other edge detection algorithms Canny delivers the best and most robust results (Mathworks, n.d.). Because the edge points obtained are not continuous, dilatation and erosion processes are performed (4) to reconstruct a continuous edge between the left and the right image border (5). The end points of the reconstructed edge are then connected by a straight line  $y_i$  (6). The average absolute distance  $R_m$  between  $y_i$  and the detected edge is calculated with pixel-to-pixel resolution and a pixel distance of  $0.5 \mu\text{m}$  (7). Note that this algorithm is well-defined even when there is a non-unique mapping of the center line to the border curve (e.g., for tilted or curved ink filaments) or when isolated ink residuals are situated close to the rim.

### 3. Results and discussion

By focusing the edges of pad-printed images we identified the so-called ‘stamp effect’, which is a typical defect occurring in pad-printing as it is also described by Hübner and Till (2007). By taking a closer look at the printing form in Figure 14, it can be clearly seen that this ‘stamp’ defect is related to the walls between the raster cells at the border of the ink transfer areas on the surface of the printing form. The raster is described in Section 1.3. The roughness measured on the printed patterns (Figure 14) is quite variable in the individual fields and ranges from  $10 \mu\text{m}$  to  $35 \mu\text{m}$ . A closer comparison with the gravure patterns of the printing form reveals that this type of defect is related to the relative gravure cells’ row distance to the geometric border of the respective field on the printing form. These walls at the border are transferred in the printing process which can be seen in Figure 14b in the printing result with a wavy contour, the ‘stamp effect’.

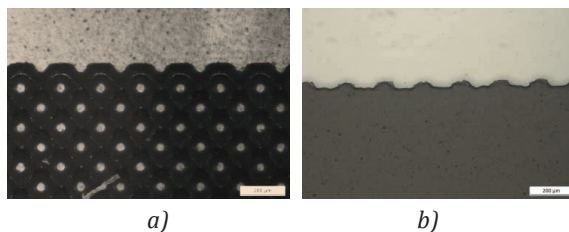
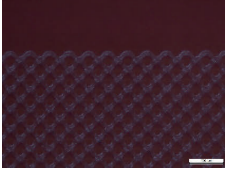
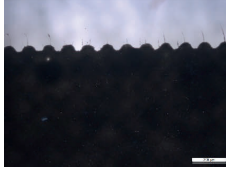
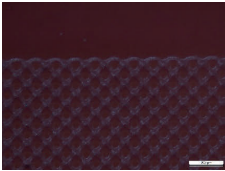
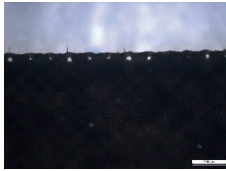


Figure 14: Ten times lens magnification images of a printing form at the border of the pattern, imaged with a two-step exposure (a), and the resulting printed image with a ‘stamp’ defect (b)

As shown in Table 1, it seems that the position of the raster walls at the edge is random. The position results from the desired layout and the fact that in the second exposure step a film fully covered with a raster is used. If rastered printing images with straight edges and without these ‘stamp’ defects are desired, so-called outlines should be used (Hahne, 2001; Kokot, 2013).

Table 1: Ten times lens magnification images of a polymer printing forms (left column) with a raster frequency of 120 L/cm at random different areas of the edges of the pattern, the resulting printed image (right column) and the measured  $R_m$  by Equation [1]

Printing form	Printed image	$R_m$ ( $\mu\text{m}$ )
		10.87
		2.45

An outline is a contour in the digital layout which is aligning inward around the layout. The requirement for the line width is that it should be slightly larger than one raster wall to eliminate it from the edge. At the same time, the line width shouldn't be too large, so that the blade cannot tilt in these areas.

In our experiments the clichés with the coarsest resolution are those with a raster frequency of 80 L/cm. Those therefore have the largest raster walls. In there, one raster wall is not larger than 50  $\mu\text{m}$ . A line width of 50  $\mu\text{m}$  for the outline turned out to be sufficient for all three used raster frequencies. Contrary to what is shown in Figure 7, where one layout film and one raster film is needed, the raster specific for this layout is then already implemented in the digital layout combined with the outline (as shown in Figure 15, right) and transferred to the film material.

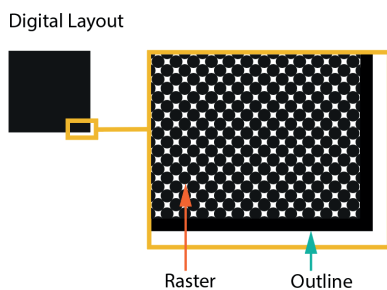


Figure 15: Digital layout for the one-step exposure with implemented raster and outline

Only one exposure step is sufficient, which we call 'one-step exposure' and will be explained later. Thus, in the printing form production (photopolymer or steel based), outlines eliminate the walls of the raster at the edges and reveal in a printed result (as shown in Figure 16b) with a straight edge.

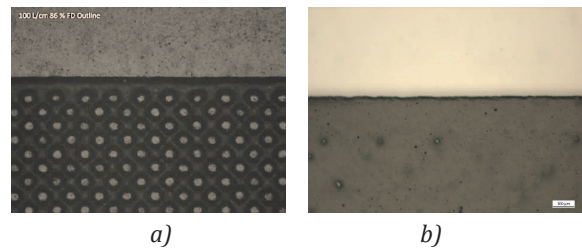


Figure 16: Ten times lens magnification image of (a) printing form with outlines, and (b) printed result with a straight edge ( $R_m = 1.76 \mu\text{m}$ )

The most commonly used process to produce printing forms, as described above in section 1.4, is a two-step exposure process, due to two films (one with the layout and one with the desired raster) that are necessary.

For implementing outlines, a 'one-step exposure' process is necessary. The difference between both processes is described below. In general, there are two possibilities to implement a raster in a printing form. Which of the variants is chosen depends on the requirements of the printing job.

A. Two-step exposure (most commonly used)

The first exposure with the image layout is followed by a second exposure with the desired raster. Different raster films are available with different raster frequencies and area coverages. The advantage here is the easy processing and the flexibility if another raster frequency is needed.

B. One-step exposure

The one-step exposure can be used if the raster is already integrated in the layout. The advantage in this process is first that only one exposure step is necessary, and second that so-called outlines can be implemented to print sharp edges. The disadvantage in this case is the comparatively more complex preparation of the data.

Table 2: Results of the printing experiments with different printing form materials, different raster frequencies and the resulting edge roughness  $R_m$ ; all used printing forms in this table have outlines

Printing form material	Raster frequency (L/cm)	$R_m$ ( $\mu\text{m}$ )
Polymer	80	2.44 ( $\pm 1.02$ )
	100	1.76 ( $\pm 0.95$ )
	120	1.50 ( $\pm 0.28$ )
Steel	80	1.74 ( $\pm 0.38$ )
	100	1.83 ( $\pm 0.48$ )
	120	1.55 ( $\pm 0.27$ )
Average		1.80 ( $\pm 0.31$ )

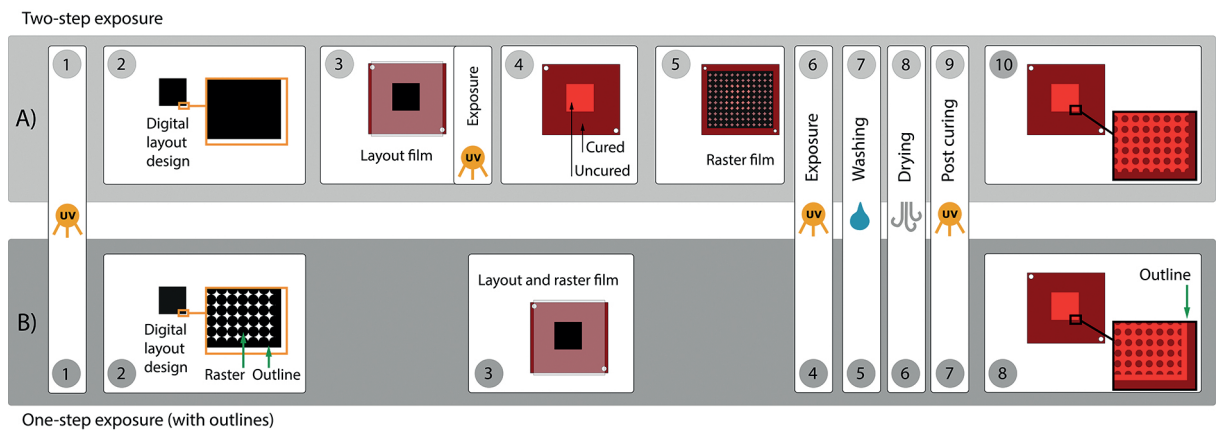


Figure 17: Schematic showing the difference between the process of the two-step exposure (A) and the one-step exposure (B)

Figure 17 shows the differences between both processes employing the two-step (A) and one-step exposure (B) to produce a pad-printing form. The resulting printing forms from both processes (A) and (B) are the same with one significant difference that in (B) outlines are included, which enables printing of sharp edges. When we replaced the printing forms with those having outlines, we achieved an average edge roughness  $R_m$  of  $1.80 \pm 0.31 \mu\text{m}$ . This represents an enormous improvement in edge quality (Table 2).

Out of the results we can see that the edge roughness is independent of printing form material and raster frequency. Raster frequency and area coverage, as well as the exposure and etching time determine the cell depth and thus also the theoretical ink volume (microPrint, 2012). The results obtained here also show that (if edge accuracies below  $3 \mu\text{m}$  are desired) raster frequency and thus the ink volume has no influence on the edge roughness as long as the outlines are used.

#### 4. Conclusion

In this work, we consider the edge quality of pad-printed structures. With the help of Matlab software we created an algorithm to measure the edge roughness. With this algorithm we measured edge rough-

ness's of more than  $10 \mu\text{m}$ . We determined within each printing sample huge deviations of the measured roughness's at different areas of the sample due to strongly varying wavy contours of the edges. These wavy contours can be traced back to the cliché, where those so-called 'stamp effects' already occur. We identify the 'stamp effect' as a printing defect when focusing on the edge roughness. 'Stamp' defects are related to the structure of the printing area of the printing cliché. By providing an outline feature, 'stamp' defects can be avoided. To do this, the printing form must be exposed with a one-step exposure instead of the two-step exposure usually used. The raster and the outline must then be accordingly created in the layout. In the experiments we printed one layout with different printing forms (photopolymer and thin steel) and different raster frequencies, which has influence to the transferred ink volume and resolution. We expected to see an influence to the edge roughness with the algorithm we created. In experiments we used clichés with implemented outlines. It turned out that the raster frequency of the printing cliché and cliché material has no influence on the edge sharpness in our experimental setup. Summarizing, with regard to the printing results and the measured edge roughness, we can say that a value of less than  $3 \mu\text{m}$  for the edge roughness can be achieved when using outlines, regardless of the printing plate material and raster frequency.

#### Acknowledgments

The authors are thankful for many helpful hints by Jürgen Vesper from Flint Group Germany GmbH and the working group Innovation Tampondruck. Our studies on pad-printing technology were achieved within the BMBF Project ELSE under grant no. 13N13079.



## References

- Al Aboud, A., Dörsam, E., Hakimi Tehrani, A. and Spiehl, D., 2018. Using FEM simulation as a tool to develop pad printing. In: P. Gane, ed. *Advances in Printing and Media Technology: Proceedings of the 45<sup>th</sup> International Research Conference of iarigai*. Warsaw, Poland, October 2018. Darmstadt, Germany: iarigai, pp. 107–114.
- Bodenstein, C., 2018. Einflüsse auf die Kantenqualität tampongedruckter Strukturen und deren Beurteilung für die Anwendung in der gedruckten Elektronik. In: *Open Seminar: Innovation Tampondruck 2018*. Bietigheim-Bissingen, Germany, 27–28 November 2018.
- Bodenstein, C., Sauer, H.M., Hirmer, K. and Dörsam, E., 2018a. Influence of printing parameters in fully pad-printed electroluminescence panels on curved surfaces. In: *19<sup>th</sup> International Coating Science and Technology Symposium (ISCST)*. Long Beach, CA, USA, 16–19 September 2018.
- Bodenstein, C., Sauer, H.M., Fernandes, F., Dörsam, E. and Warsitz, E., 2018b. Assessing the quality of pad-printed images by evaluating edge sharpness. In: P. Gane, ed. *Advances in Printing and Media Technology: Proceedings of the 45<sup>th</sup> International Research Conference of iarigai*. Warsaw, Poland, October 2018. Darmstadt, Germany: iarigai, pp. 97–106.
- Canny, J., 1986. A computational approach to edge detection. *IEEE Transactions on Pattern Analysis and Machine Intelligence*, 8(6), pp. 679–698. <https://doi.org/10.1109/TPAMI.1986.4767851>.
- Hahne, P., 2001. *Innovative Drucktechnologien: Siebdruck – Tampondruck*. Lübeck, Germany: Der Siebdruck, p. 94.
- Hahne, P., Hirth, E., Reis, I.E., Schwichtenberg, K., Richtering, W., Horn, F.M. and Eggenweiler, U., 2001. Progress in thick-film pad printing technique for solar cells. *Solar Energy Materials and Solar Cells*, 65(1), pp. 399–407. [https://doi.org/10.1016/S0927-0248\(00\)00119-7](https://doi.org/10.1016/S0927-0248(00)00119-7).
- Hakimi Tehrani, A., 2018. *Automation improvement of indirect gravure printing with a focus on the mechanical characteristics of silicone rubber pads*. PhD Thesis. Technische Universität Darmstadt.
- Hakimi Tehrani, A., Dörsam, E. and Neumann, J., 2016. Improving automation and process control of an indirect gravure (pad) printing machine. *Acta Polytechnica Hungarica*, 13(4), pp. 221–240.
- Hübner, G. and Till, W., 2007. Rotogravure and pad printing of microstructures for electronic applications like oFETs. In: N. Enlund and M. Lovreček, eds. *Advances in Printing and Media Technology: Proceedings of the 34<sup>th</sup> International Research Conference of iarigai*. Grenoble, France, 9–11 September 2007. Zagreb, Croatia: Acta Graphica Publishers, pp. 297–305.
- Kokot, J., 2013. *Drucken und Veredeln im Bogentiefdruck: Verpackungs- und Etikettendruck mit Verfahrenskombinationen*. Esslingen, Germany: Bibliothek des grafischen Wissens, p. 47.
- Krebs, F.C., 2009. Pad printing as a film forming technique for polymer solar cells. *Solar Energy Materials and Solar Cells*, 93(4), pp. 484–490. <https://doi.org/10.1016/j.solmat.2008.09.003>.
- Lake, M., 2017. *Oberflächentechnik in der Kunststoffverarbeitung: Vorbehandeln, Beschichten, Bedrucken, Funktionalisieren, Prüfen*. Munich, Germany: Carl Hanser Verlag, p. 302.
- Lee, T.-M., Hur, S., Kim, J.-H. and Choi, H.-C., 2010. EL device pad-printed on a curved surface. *Journal of Micromechanics and Microengineering*, 20(1):015016. <https://doi.org/10.1088/0960-1317/20/1/015016>.
- Leppävuori, S., Väänänen, J., Lahti, M., Remes, J. and Uusimäki, A., 1994. A novel thick-film technique, gravure offset printing, for the realization of fine-line sensor structures. *Sensors and Actuators A: Physical*, 42(1–3), pp. 593–596. [https://doi.org/10.1016/0924-4247\(94\)80060-X](https://doi.org/10.1016/0924-4247(94)80060-X).
- Mathworks, n.d. *Edge Detection*. [online] Available at: <<https://de.mathworks.com/help/images/edge-detection.html>> [Accessed 10 January 2018].
- Merilampi, S.L., Björninen, T., Ukkonen, L., Ruuskanen, P. and Sydänheimo, L., 2011. Characterization of UHF RFID tags fabricated directly on convex surfaces by pad printing. *The International Journal of Advanced Manufacturing Technology*, 53(5–8), pp. 577–591. <https://doi.org/10.1007/s00170-010-2869-y>.
- microPrint, 2012. *The pad printing book*. [pdf] Schaffhausen, Switzerland: microPrint LC GmbH. Available at: <<http://www.microprint.ch/pdf/The-pad-printing-book.pdf>> [Accessed 06 December 2018], p. 43.
- Mooring, L., Karousos, N.G., Livingstone, C., Davis, J., Wildgoose, G.G., Wilkins, S.J. and Compton, R.G., 2005. Evaluation of a novel pad printing technique for the fabrication of disposable electrode assemblies. *Sensors and Actuators B: Chemical*, 107(2), pp. 491–496. <https://doi.org/10.1016/j.snb.2004.11.005>.
- Nisato, G., Lupo, D. and Ganz, S. eds., 2016. *Organic and Printed Electronics. Fundamentals and Applications*. Boca Raton, FL, USA: Pan Stanford Publishing, CRC Press, pp. 70–71.
- Willfahrt, A., 2007. Examination of the printability of microstructures by means of pad printing for the realization of minimal structures for the use of conductive inks on PET-Substrate. In: *Printing Future Days 2007: Proceedings of the 2<sup>nd</sup> International Student Conference on Print and Media Technology*. Chemnitz, Germany, 5–8 November 2007. Berlin, Germany: Verlag für Wissenschaft und Forschung.
- Xiong, Y. and Qu, Z., 2011. Antenna 3D pad printing solution evaluation. In: *International Symposium on Antennas and Propagation (APSURSI)*. Spokane, WA, USA, 3–8 July 2011. New York, NY, USA: IEEE, pp. 2773–2776. <https://doi.org/10.1109/APS.2011.5997101>.

